Journal of Applied Mechanics and Technical Physics, Vol. 36, No. 4, 1995

MATHEMATICAL MODELING OF THE SLIDER–DISK INTERACTION IN DISK UNITS OF THE WINCHESTER TYPE

R. A. Gruntfest

UDC 532.516

The main elements of disk units are a rotating disk and a magnetic head (slider) sliding at a small altitude over the disk surface. A thin air layer prevents contact between the slider and the disk and creates conditions for the stable flight of the slider at a given altitude. Obviously, mathematical modeling of the slider–air layer–disk system is an indispensable step in the general program of disk unit design. There are no systematic investigations on this topic in Russia. Foreign publications over the last 5–7 years bear witness to the extensive theoretical studies on this topic, but they do not contain full information, and most of all, do not contain program realization, and therefore cannot be considered "know how" [1–3].

Three problems were distinguished in the theoretical consideration: 1) stationary flight of the slider; 2) slider dynamics under periodical and shock external actions and during transition between the tracks; 3) contact interactions between the slider and the disk in the processes of taking off and landing. The present paper deals with the first two problems.

The geometry of a standard slider is shown in Fig. 1, where U, V are the longitudinal and transversal velocities of the slider relative to the disk; a, b, c, d, and e are the geometrical parameters of the slider; ψ_0 is the attack angle; ψ_1, ψ_2 are the slope angles of the slider relative to the disk plane; ψ_3 is the rotation angle of the slider in the disk plane; m, J_1, J_2, J_3 are the mass and inertia momenta of the slider; F, M_1, M_2, M_3 are the force and force momenta acting on the head from the elastic bearing; P, L_1, L_2, L_3 are the aerodynamic force and force momenta, applied to the head from the air layer side; x_F, y_F is the application point of the elastic force F; and $h(x, y, t)$ is the air layer thickness (clearance).

The nonstationary flow of a viscous gas in a thin layer taking into account the molecular sliding on the boundary surfaces is described by the Reynolds equation [4, 5]

$$\mathrm{Sh}\,\frac{\partial(h(1+p))}{\partial t} + \frac{\partial(h(1+p))}{\partial x} + \beta\,\frac{\partial(h(1+p))}{\partial y} = \varepsilon\frac{\partial}{\partial x}\Big[h^2(h+\alpha+hp)\frac{\partial p}{\partial x}\Big] + \delta\frac{\partial}{\partial y}\Big[h^2(h+\alpha+hp)\frac{\partial p}{\partial y}\Big]. \quad (1)$$

Here $p(x, y, t)$ is the sought function denoting the dimensionless excessive pressure in the air layer; $\mathrm{Sh} = 2a/U\tau$ is the Strouhal number; $\varepsilon = h_0^2 p_0/6\mu U a$ is the compression number; $\alpha = 6\lambda_0/h_0$ is the coefficient of sliding; $\beta = aV/bU$; $\delta = (a/b)^2\varepsilon$; p_0 is the air pressure in the disk unit volume; μ is the air viscosity; λ_0 is the free path length of molecules; h_0 is the clearance in the outlet section; and τ is the time scale defined below.

The boundary conditions for Eq. (1) are

$$\begin{aligned} p = 0 \quad &\text{at} \quad x = 0, \ x = 1, \\ p = 0 \quad &\text{at} \quad y = 0, \ y = 1. \end{aligned} \quad (2)$$

The thickness of the air layer (taking into account the attack angle at the entrance) is given by

$$\begin{aligned} h(x,y,t) &= h(t) + \psi_0(t)(d/a - x) + \psi_1(t)(1-x) \mp \psi_2(t)(c/2a - y), \quad 0 \leqslant x < d/a, \\ h(x,y,t) &= h(t) + \psi_1(t)(1-x) \mp \psi_2(t)(c/2a - y), \quad d/a \leqslant x \leqslant 1, \quad 0 \leqslant y \leqslant 1. \end{aligned} \quad (3)$$

The upper sign in (3) corresponds to the outer ski of the slider; the lower one corresponds to the inner ski. The solution of the complicated boundary value problem (1)–(3) is obtained by the finite-element method (FEM).

Rostov State University, Rostov-on-Don 344000. Translated from Prikladnaya Mekhanika i Tekhnicheskaya Fizika, Vol. 36, No. 4, pp. 45–51, July–August, 1995. Original article submitted July 21, 1993; revision submitted July 25, 1994.

0021-8944/95/3604-0520 $12.50 © 1996 Plenum Publishing Corporation

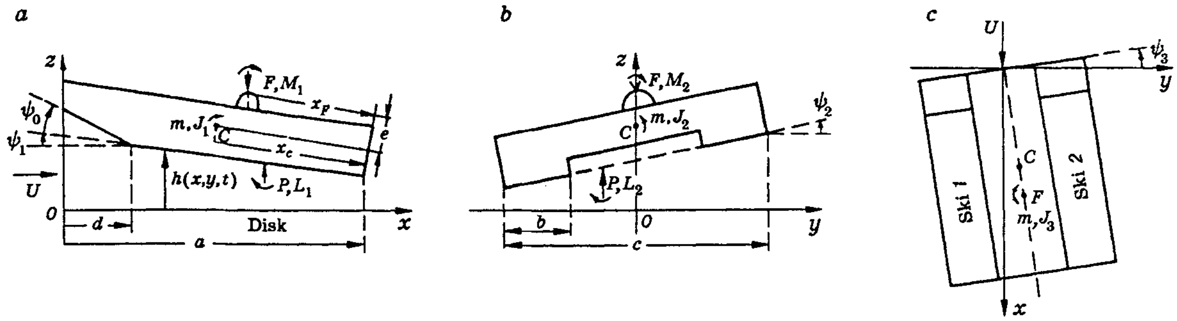

Fig. 1

The flow region is divided into rectangular cells (elements). The pressure variables $p_{ij}(t)$ are introduced in the nodes, after which the following approximations are used:

$$p(x,y,t) = \sum_{i=1}^{n1}\sum_{j=1}^{n2} p_{ij}(t)\,\omega_i(x)\,\omega_j(y), \qquad p^2(x,y,t) = \sum_{i=1}^{n1}\sum_{j=1}^{n2} p_{ij}^2(t)\,\omega_i(x)\,\omega_j(y), \tag{4}$$

where $\omega_i(x)$ are the Courant functions of the "hat" kind; $n1, n2$ are the numbers of the internal nodes along the x and y axes respectively. Representations (4) take into account boundary conditions (2). The standard FEM procedure applied to Eq. (1) yields a system of nonlinear ordinary differential equations

$$\frac{d}{dt}P_{rq} = \sum_{i=1}^{n1}\sum_{j=1}^{n2}(L_{ij}^{rq}\,p_{ij} + Q_{ij}^{rq}\,p_{ij}^2) - R_{rq}, \quad 1 \leqslant r \leqslant n1, \quad 1 \leqslant q \leqslant n2. \tag{5}$$

The elements of the L and Q matrices are rather cumbersome and are omitted here. For numerical integration of (5) by means of the Runge–Kutta method, it is necessary to specify initial conditions. If the motion of the slider begins from a certain stationary state, the corresponding stationary pressure distribution in the nodes should be taken as the initial conditions:

$$p_{ij} = p_{ij}^{(0)} \quad \text{at} \quad t = 0. \tag{6}$$

The system (5) of differential equations can be used for studying the stationary flight or periodical motion of the slider by the stationarity method. In these cases one can specify zero initial conditions for the pressure

$$p_{ij} = 0 \quad \text{at} \quad t = 0, \tag{7}$$

and solutions to the formulated problems are to be obtained at $t \to \infty$. Stationary flow can also be examined with the help of a system of nonlinear algebraic equations:

$$\sum_{i=1}^{n1}\sum_{j=1}^{n2}(L_{ij}^{rq}\,p_{ij} + Q_{ij}^{rq}\,p_{ij}^2) = R_{rq}, \quad 1 \leqslant r \leqslant n1, \quad 1 \leqslant q \leqslant n2. \tag{8}$$

We shall construct its solution by means of Newton's iteration method, taking conditions (7) as an initial approximation. The pressure found in the nodes allows one to determine the lifting aerodynamic force and force moments that act on the slider from the side of the air layer:

$$P(t)/p_0\,a\,b = \int_0^1\!\!\int_0^1 p\,dx\,dy = \sum_{i=1}^{n1}\sum_{j=1}^{n2} p_{ij}\,\sigma_{ij}/4,$$

$$L_1/p_0\,a^2\,b = \int_0^1\!\!\int_0^1 (1-x)\,p\,dx\,dy = \sum_{i=1}^{n1}\sum_{j=1}^{n2} p_{ij}\,(1-x_i)\,\sigma_{ij}/4,$$

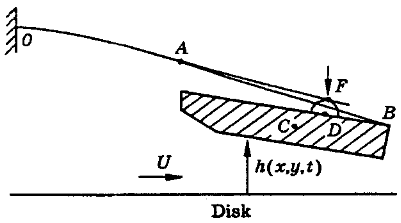

Fig. 2

$$L_2/p_0\,a\,b^2 = \int_0^1\int_0^1 y\,p\,dx\,dy = \sum_{i=1}^{n1}\sum_{j=1}^{n2} p_{ij}\,y_j\,\sigma_{ij}/4,$$

$$L_3 = ((V + U\,\psi_3)æ_1 - a\,\dot{\psi}_3\,æ_2)\mu\,a^2\,b/h_0 - \psi_2(L_1 - P\,x_F)/2,$$

$$æ_i = \int_0^1\int_0^1 \frac{(x_F - x)^i}{h(x,y,t) + \alpha/3}dx\,dy \quad (i = 1, 2).$$

Here (x_i, y_j) are the (i,j)-th node coordinates, and σ_{ij} is the area of finite elements.

The access arm (elastic bearing) sets the slider on a definite track and provides the pressing force F_0, which acts at the point (x_F, y_F). The bearing schematic is shown in Fig. 2, where OAF is an elastic console beam, AB is an elastic beam fixed at both ends, and DF is a stiff spherical joint. The bearing provides four degrees of freedom of the slider, namely, the vertical shift $h(t)$ and the rotation angles $\psi_1(t)$, $\psi_2(t)$, $\psi_3(t)$ relative to the x, y, and z axes. The arm is calculated by methods of material resistance with regard for simultaneous translations at points F and D. This allows one to obtain the following equations for the slider motion under the action of aerodynamic and elastic forces:

$$\begin{aligned} &\widetilde{m}\,\ddot{h} + \tilde{s}_A\,\ddot{\psi}_1 = P - F - \widetilde{m}\,g\,k_1(t), &&\tilde{s}_A\,\ddot{h} + \tilde{j}_A\,\ddot{\psi}_1 = L_1 - M_1 - \tilde{s}_A\,g\,k_1(t), \\ &J_2\,\ddot{\psi}_2 = L_2 - M_2 - k_2(t)mge, &&J_3\ddot{\psi}_3 = L_3 - M_3 - k_2(t)m\,g(x_C - x_F). \end{aligned} \tag{9}$$

Here $\widetilde{m}$, $\tilde{s}_A$, and $\tilde{j}_A$ are the reduced mass, static, and inertia moments relative to point A for the bearing–slider system; $k_i(t)$ are the overload coefficients along the z and y axes ($i = 1, 2$); $M_1 = F_0 x_F + hC_{10} + \psi_1 C_{11}$; $M_2 = C_2\psi_2 + F_0 y_F$; $M_3 = C_3\psi_3$ (C_0, C_{10}, C_{11}, C_2, C_3 are the effective stiffnesses of the bearing which can be either calculated or found experimentally).

Since the aerodynamic forces depend essentially on the slider motion, systems (5) and (9) of differential equations should be combined and integrated together, and initial conditions (6) should be supplemented by the following ones:

$$h = h_0, \quad \dot{h} = h_1, \quad \psi_i = \psi_{i0}, \quad \dot{\psi}_i = \psi_{i1} \quad (i = 1, 2, 3) \quad \text{at} \quad t = 0,$$

where h_0, ψ_{i0} are the parameters of the initial position from which the slider motion begins; h_1, ψ_{i1} are the initial linear and rotation velocities, caused by shock actions on the slider. For the stationary problem we obtain from (9) the algebraic system

$$P - F - \widetilde{m}\,g\,k_1 = 0, \quad L_1 - M_1 - \tilde{s}_A\,g\,k_1 = 0,$$
$$L_2 - M_2 - k_2\widetilde{m}\,g\,e = 0, \quad L_3 - M_3 - k_2\,m\,g\,(x_C - x_F) = 0,$$

which should also be combined with system (8) and solved jointly by Newton's iteration method. However, specifying an initial approximation presents difficulties and requires certain skill.

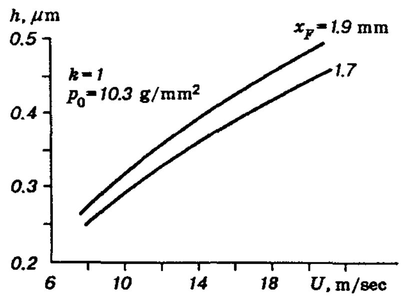

Fig. 3

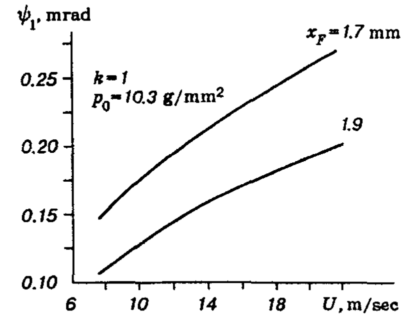

Fig. 4

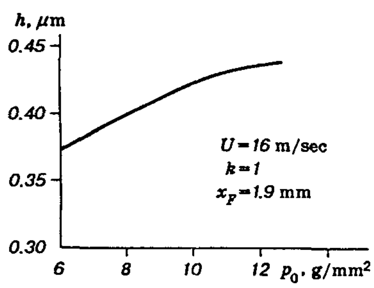

Fig. 5

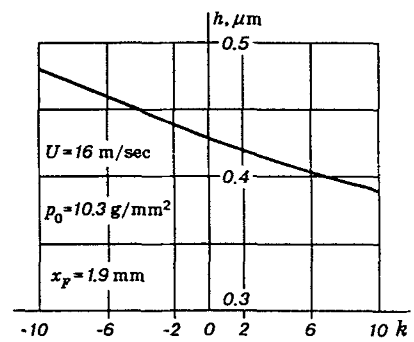

Fig. 6

The algorithms proposed for solving the stationary and dynamic problems have been performed as a PC program package. These programs can be used both for calculating sliders of existing constructions and for designing new types of sliders. Let us discuss some results for a slider with the following parameters (see Fig. 1):

$$a = 4 \text{ mm}, \quad b = 0.65 \text{ mm}, \quad c = 3.35 \text{ mm}, \quad d = 0.4 \text{ mm}, \quad e = 0.65 \text{ mm},$$

$$m = 0.074 \text{ g}, \quad J_1 = 0.4 \text{ g}\cdot\text{mm}^2, \quad J_2 = 0.07 \text{ g}\cdot\text{mm}^2, \quad J_3 = 0.17 \text{ g}\cdot\text{mm}^2,$$

$$\widetilde{m} = 0.091 \text{ g}, \quad \tilde{s}_A = 0.182 \text{ g}\cdot\text{mm}, \quad \tilde{J}_A = 0.47 \text{ g}\cdot\text{mm}^2,$$

$$C_0 = 1.5 \text{ g/mm}, \quad C_{10} = 4.5 \text{ g}, \quad C_{11} = 42 \text{ g}\cdot\text{mm/rad}, \quad C_2 = 40 \text{ g}\cdot\text{mm/rad},$$

$$F_0 = 10 \text{ g}, \quad x_C = 2 \text{ mm}, \quad y_F = 0, \quad \psi_0 = 15 \text{ mrad}.$$

The physical parameters of the air in the disk unit chamber are as follows:

$$\mu = 0.00018 \text{ P}, \quad \lambda_0 = 0.069 \ \mu\text{m}, \quad p_0 = 10.3 \text{ g/mm}^2.$$

In Figs. 3 and 4, the output clearance h and the slope angle ψ_1 are plotted as functions of the disk velocity for two positions of the force application point $x_F = 1.9$ and 1.7 mm ($y_F = 0$ for both cases). The shift of the force application point toward the outlet section increases the angle ψ_1 and decreases the clearance. In the real region of the flight velocities 10–20 m/sec, the relative slot variation is within 40%.

Figures 5 and 6 can be useful in analyzing the disk unit operation under nonstandard conditions (on mobile and high-altitude objects). Figure 5 presents the clearance variation as a function of the pressure inside the camera, and Fig. 6 shows the dependence of the slot on the overload coefficient along the z axis. In both

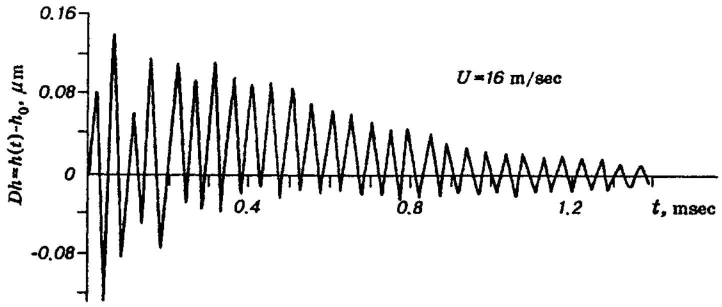

Fig. 7

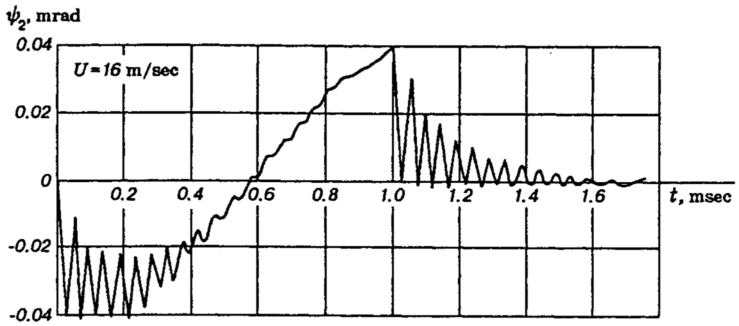

Fig. 8

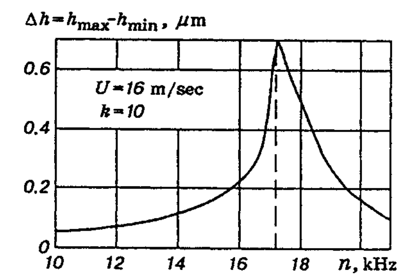

Fig. 9

cases one can conclude that the altitude of the slider flight remains normal over a wide range of variations of the corresponding parameters.

The slider dynamics under shock actions is shown in Fig. 7. The initial state is the stationary flight of the slider at a velocity of 16 m/sec, which corresponds to $h = 0.42$ μm, $\psi_1 = 0.17$ mrad, $\psi_2 = 0$, $\psi_3 = 0$. On account of a shock pulse, the slider gains the initial velocities $\dot{h} = 10$ mm/sec, $\dot{\psi}_1 = 5$ rad/sec, $\dot{\psi}_2 = 10$ rad/sec. By virtue of the energy dissipation in a viscous gas, the slider oscillation amplitude is damped with time. The duration of the transient stage, after which the amplitude decreases by an order of magnitude relative to the maximal one, is about 1 msec. This important quantity characterizes the time it takes for the slider to return to normal operation. Also, note the high frequency vibration of the slider with a period $\tau = 55$ μsec, which does not depend on the intensity of the initial perturbation and is the period of natural oscillations of the bearing–slider–air layer–disk system. Despite a rather strong shock, no collision occurs between the slider and the disk since the flight velocity is high enough. But at low velocities of the slider during taking off and landing, the stiffness of the air layer significantly decreases, resulting in collisions between the slider and the disk.

Figure 8 shows the slope angle oscillations $\psi_2(t)$ caused by transitions of the slider between tracks. Here the particular case where the force application point coincides with the mass center of the slider ($x_F = x_C$, the rotation angle $\psi_3 = 0$) is calculated. The change in transversal velocity is taken in the form $V = 0.157 \sin(\pi t)$ m/sec, which corresponds to a transition time of 1 msec and a distance between the tracks of 100 μm. The acceleration leaps at the initial and finite moments ($50g$) excite the damping oscillations of the slider, whose amplitude decreases by one order of magnitude per 0.5 msec (decrement about 0.8).

Figure 9 shows the influence of periodic perturbations (vertical vibration of the whole system) on the slider clearance magnitude. Here the dependence of the oscillation amplitude on the vibration frequency (maximum overload $10g$) is shown. As might be expected, the curve maximum corresponds to the frequency of free oscillations mentioned above (18,000 Hz). The forced oscillations at this frequency (including those of sound origin) are the most dangerous for the slider normal operation.

Of course, these results do not give a complete analysis of the slider behavior under various conditions and only illustrate the potentialities of the theory and program, which are offered to interested persons and organizations.

REFERENCES

1. C. Garsia-Suarez, D. E. Bogy, and F. E. Talke, "Use of an unwind finite element scheme for air-bearing calculation," *Tribology Mech. Magn. Storage Systems*, SP-16, 390–396 (1984).
2. Y. Yamaguchi, K. Takashi, H. Fujita, and K. Kuwachara, "Flow induced vibration of magnetic recording disks," *IEEE Trans. Magn.*, No. 5, 1022–1024 (1986).
3. R. Benson, C. Chiang, and F. Talke, "The dynamics of slider bearings during contacts between slider and disk," *IBM J. Res. Dev.*, **33**, No. 1 (1989).
4. C. A. Sheinberg, *Sliding Supports with a Gas Lubricant* [in Russian], Mashinostroenie, Moscow (1979).
5. N. S. Slezkin, "Reynolds equations for gas lubricant flow with regard for the sliding of the first and second order," *Vestn. MGU*, Ser. 1, No. 6 (1981).
6. G. I. Marchuk, *Methods of Computing Mathematics* [in Russian], Nauka, Moscow (1989).